DTU Library

Modelling of composite concrete block pavement systems applying a cohesive zone model

Skar, Asmus; Poulsen, Peter Noe

Publication date:
2015

Document Version
Peer reviewed version

[Link back to DTU Orbit](#)

Modelling of composite concrete block pavement systems applying a cohesive zone model

Asmus Skar*— Peter Noe Poulsen**

COWI A/S, Parallelvej 2, 2800 Kgs. Lyngby, Denmark
asch@cowi.dk

** *Technical University of Denmark, Department of Civil Engineering, Brovej, Bygning 118, 2800 Kgs. Lyngby, Denmark*
pnp@byg.dtu.dk

ABSTRACT: *This paper presents a numerical analysis of the fracture behaviour of the cement bound base material in composite concrete block pavement systems, using a cohesive zone model. The functionality of the proposed model is tested on experimental and numerical investigations of beam bending tests. The pavement is modelled as a simple slab on grade structure and parameters influencing the response, such as analysis technique, geometry and material parameters are studied. Moreover, the analysis is extended to a real scale example, modelling the pavement as a three-layered structure. It is found that the cohesive model is suitable for simulation of crack propagation in cement bound materials subjected to monotonic loading. The methodology implemented gives a new understanding of the mechanical behaviour of cement bound materials which can be used in further refinements of mechanical models for composite block pavements. It is envisaged that the methodology implemented in this study can be extended and thereby contribute to the ongoing development of rational failure criteria that can replace the empirical formulas currently used in pavement engineering.*

KEYWORDS: *cement bound material fracture, cohesive zone model, composite block pavements, pavement analysis, finite element modelling*

1. Introduction

Ports- and industries require special types of pavements to resist the heavy static loads from containers. Typically, concrete block pavement systems are applied over a stiff layer of cement bound material to reduce the risk of rutting and settlements over time.

The structural design and evaluation of such pavements is traditionally based on a phenomenological approach for description of the damage in quasi-brittle cemented layer. The method is practical and simple because it gives the user direct analytical expressions. However, such empirically based material models have limited applicability and deals with a limited number of materials in a restricted range of design options. This type of model does not distinguish between crack initiation and crack propagation or elastic and inelastic work, model parameters are simply regression constants without direct physical meaning.

To increase the versatility of the existing methods and move toward a more rational approach in design of concrete block pavement systems this paper evaluates the applicability of a simplified fracture mechanics model to predict the response of the pavement structure. The aim of this approach is to create a link and coherence in between laboratory, design and field applications. To obtain this goal, it is necessary to test on actual physical properties and include mechanical models in characterization and modelling of materials.

The overall idea of the specific problem is that the primary structural response in a simplified three-layered composite block pavement structure is controlled by the degradation of the cement bound material (CBM), and that this nonlinear response, mainly can be explained by the fracture behaviour, which is imagined to occur in similar fashion to a yield line mechanism. Crack propagation and stiffness reduction of the CBM further leads to increased stresses in the underlying sub-base and subgrade, which again lead to permanent deformations.

The present study deals with a simplified framework for description of the degradation of the composite pavement, considering two orthogonal discrete cracks in the CBM-layer under interior static load only. The discrete crack method has been frequently applied in numerical analysis of quasi-brittle materials, e.g., concrete.

2. Methodology

2.1 Model idealizations

To improve the understanding of fracture behaviour of CBM a discrete crack model is chosen for the present study based on the fictitious crack model (FCM) originally developed by Hillerborg (1976). This means that for the fracture process, built-in traction separation based cohesive contact surfaces is inserted along the anticipated fracture plane in the CBM layer in the orthogonal directions as per Meda (2004). This is deemed a reasonable model at the edge and interior of CBM-layer, since the fracture plane is anticipated in the direction of the maximum stress.

Previous large-scale studies, e.g., Shahid and Thom (1996), Theyse et. al. (1996), Thøgersen et. al. (2006) and Yeo (2008*a*), indicate that cracks are initiated at the bottom of the CBM layer, before propagating where after it propagates upwards through the layer thickness, corresponding to an opening mode (*Mode I*) type of cracking. Thus, for the present study *Mode I* type of cracking is assumed, as the

contribution of the shear stresses is expected to be negligible. A simple three-layered structure with concrete block pavers (CBP) and bedding layer over CBM and subgrade soil is considered for monotonic interior loading.

In this study, commercial general purpose FE program ABAQUS/Standard®, version 6.13-1 is employed in the analysis of the pavement structure.

2.2 Material law

The FCM assumes that the traction stress is purely a material property, independent of specimen geometry and size. The softening curve that relates the traction stress to the opening displacement, i.e. describe the rate at which the material stiffness degrades after the damage initiation criterion is reached, is defined in terms of the total fracture energy, G_F, the material tensile strength, f_t , and the shape of the softening curve. The total fracture energy, G_F, needed to produce a stress-free crack given as the area under the curve, i.e.:

$$G_F = \int_0^{w_c} \sigma \, dw \qquad [1]$$

where w_c is the crack opening displacement and t is the corresponding traction stress. For the linear softening curve this gives a final zero-traction displacement, w_c:

$$w_c = \frac{2 \times G_F}{f_t} \qquad [2]$$

The cohesive contact model in ABAQUS was selected to save computational time; enabling the use of symmetry conditions and application of a coarser mesh for the cohesive zone.

The constitutive law for cohesive contact in ABAQUS (2013) are described in terms of contact stress- and separation, i.e., $t_n = F/A$ and w_n respectively, where F is the contact force and A is the current area at each contact point. The traction stress vector, $\boldsymbol{t}$, consists of three components: t_n, t_s, and t_s, which represent the normal and the two shear tractions respectively. The corresponding separations are denoted by: w_n, w_s, and w_s. The elastic behaviour can then be written as:

$$\begin{Bmatrix} t_n \\ t_s \\ t_t \end{Bmatrix} = \begin{bmatrix} K_{nn} & K_{ns} & K_{nt} \\ K_{sn} & K_{ss} & K_{st} \\ K_{tn} & K_{ts} & K_{tt} \end{bmatrix} \begin{Bmatrix} w_n \\ w_s \\ w_t \end{Bmatrix} = \boldsymbol{Kw} \qquad [3]$$

where $\boldsymbol{K}$ is the nominal stiffness (also referred to as the penalty stiffness) and t is the contact stress, in the normal and two shear directions, respectively. If uncoupled traction is assumed (as in this study), the off-diagonal terms in the equation above are zero.

Following the onset of the crack and for as long as the strength of the cohesive zone exceeds that of the intact material, damage evolves based on the scalar stiffness degradation variable, D, defined as:

$$D = 1 - \frac{\sigma(w)}{\bar{t}_n} \qquad For \quad w_0 \leq w \geq w_c \qquad\qquad [4]$$

where $\sigma(w)$ is the contact stress for separation w, along the softening curve; $\bar{t}_n$ is the contact stress that would have corresponded to w had the pre-crack stiffness endured.

3. Verification of cohesive contact model

3.1 Preliminary evaluation of the proposed model

Several types of softening have been applied by other researchers for the description of the post-peak behaviour of quasi-brittle materials. Roesler et. al. (2007) applied user defined element (UEL) with bilinear softening in ABAQUS simulating the fracture behaviour of plain concrete beams. Gaedicke and Roesler (2009) investigated the behaviour of slabs on grade both numerically and experimentally. In both studies notched three-point bending (TPB) beam tests was used to evaluate the type of softening law and it was found, that a bilinear or exponential softening law is best suited for the description of the cohesive softening in plain concrete.

Similarly to the built-in cohesive element, bilinear softening can be handled by contact in ABAQUS, e.g., through a tabular damage function (damage versus inelastic displacement). The simulation results by Roesler (2007) using user defined cohesive elements, and Gaedicke (2009) using the built-in COH2D4 element in ABAQUS are compared to results using ABAQUS contact formulation for the cohesive zone to ensure functionality of the proposed model. The comparison between models can be seen on the load-crack mouth opening displacement (CMOD) diagram to the left in Figure 1. Beam geometry, average material properties and model parameters applied in the three independent studies can be seen in Table 1.

Table 1. *Beam geometry, average material properties and model parameters used in the numerical study of TPB tests carried out by Roesler (2007).*

	Roesler (2007)	Gaedicke (2009)	This study
Mesh size cohesive zone	~2 mm	~2 mm	~2 mm
Geometry (mm)	700x150x80	700x150x80	700x150x80
Beam span (mm)	600	600	600
Element type(s)	CSP4 UEL	CSP4 COH2D4	CSP4
Modulus of elasticity (MPa)	32,040	32,040	32,040
Poisson's ratio	0.15	0.15	0.15
Penalty stiffness (MPa)	8,430,000	100,000	32,040
Tensile strength (MPa)	4.15	4.15	4.15
Fracture Energy (N/mm)	0.164	0.164	0.164

Aure (2012) compared the response of linear softening cohesive elements to the application of the slab on grade simulations and experiments conducted by Gaedicke (2009). From these results Aure (2012) concludes that the type of softening law,

cohesive zone width and mesh do not influence the slab on grade response significantly, seen in the graph to the right in Figure 1.

(a)　　　　　　　　　　　　　　　(b)
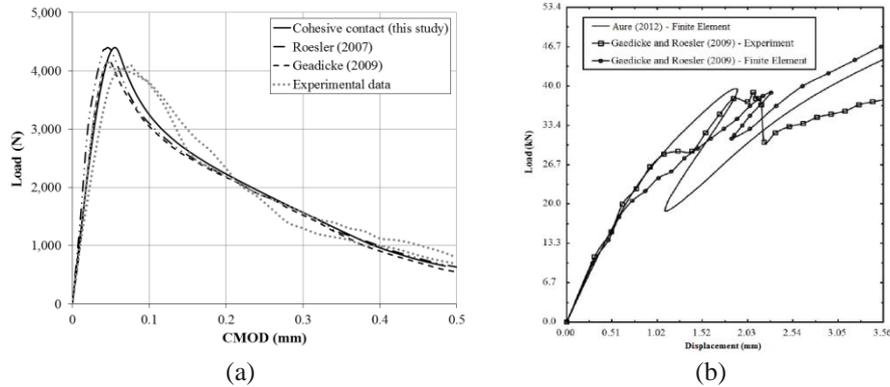
Figure 1. *(a) TPB tests on concrete (Table 1): comparison between proposed contact cohesive model, cohesive models previously applied by other independent researchers. (b) Comparison between linear and bilinear softening laws applied for slab on grade simulations compared to experimental results (Aure 2012)*

From Figure 1 it can be observed that adequately good agreement with experimental and other numerical results is obtained with the bilinear contact softening law in ABAQUS.

3.2 Numerical analysis of four-point bending tests with cement bound material

Numerical analysis of four-point bending (FPB) beam tests is carried out to verify the functionality of the cohesive contact model to simulate the fracture behaviour of crushed quartzite siltstone aggregates (D_{max}=20 mm) stabilized with GP cement (4%). Five CBM-beams (0.40×0.10×0.10 m^3) was cut from field and tested under monotonic load in a comprehensive study of CBM conducted by Austroads (Yeo 2008*b*). The strength properties were determined from specimens extracted from field slabs, shown in Table 2.

Table 2. *Average material properties and model parameters used in the numerical analysis of FPB test carried out by Austroads (Yeo, 2008b). Five beams cut from field tested.*

	Austroads beam
Modulus of elasticity (MPa)	12,760
Poisson's ratio	0.20
Penalty stiffness (MPa)	127,600
Predicted mean compression strength (MPa)	7.3
Tensile strength (MPa)	1.0
Fracture energy (N/mm)	0.028
Softening	Linear (contact)

In Table 2 the fracture energy is calculated using the correlation formula between compression strength and fracture energy suggested by Hilsdorf and Brameshuber (1991).

The beam is modelled with 2-D plain stress elements (CSP4I) in ABAQUS. A total of 840 elements are used to represent the elastic material, separated by pre-

determined contact surfaces, representing the cohesive zone (5 mm size elements), in the vertical plane at the mid-beam position.
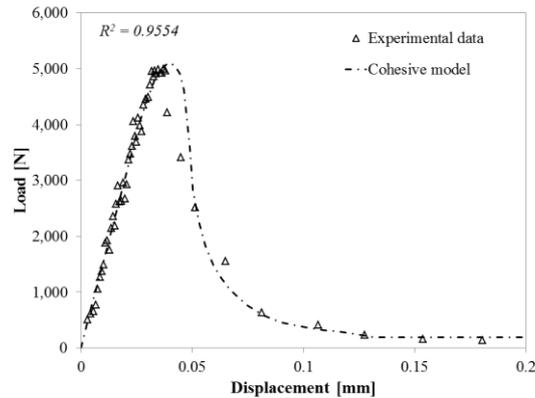
Figure 2. *Comparison between experimental data of CBM-beams and numerical cohesive model with linear softening for 4-point bending tests carried out by Austroads (Yeo 2008b)*

From the comparison between experimental and numerical results, shown in Figure 2, it can be observed that good agreement is obtained applying the cohesive model for simulation of the load-displacement response of the four-point bending beams. Relatively few data-points were obtained on the post-peak failure curve as no horizontal clip-gage control was applied during testing. The results show that a linear softening law is suitable to the description of fracture in cement bound granular mixtures. It is also found that the fracture energy of the cement bound granular mixture in this case can be predicted without further calibration, based on simple scaling with regard to compressive strength or code standards for concrete materials.
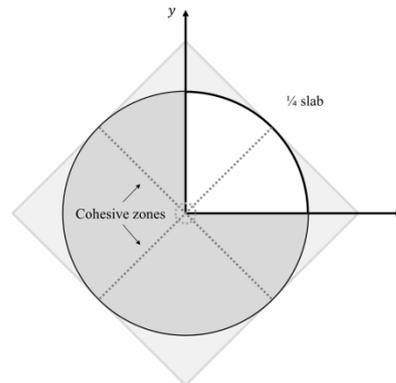
4. Sensitivity studies

To investigate the influences of geometry and variation in important material properties a sensitivity study is carried out. Preliminary investigations were used to evaluate the effect from model- and solver technique and symmetry conditions. Fixed model- and material properties used in the sensitivity study presented in this section can be seen in Table 3. The average material properties are selected to represent a typical $C_{8/10}$-material (BS, 2013), commonly applied in ports- and industries composite block pavements.

Table 3. *Model parameters and average material properties used in sensitivity study of geometrical properties*

	Fixed parameters
Mesh size cohesive zone	~10 mm
Element type	CSP3D4
Viscous stabilization factor	0.0001
Modulus of elasticity (MPa)	15,000
Poisson's ratio	0.20
Penalty stiffness (MPa)	150,000
Tensile strength (MPa)	0.8
Fracture energy (N/mm)	0.0225
Softening	Linear (contact)
Solver technique	*arc-length* (Riks, 1979)

For all subjacent models presented in this section the CBM layer over elastic foundation is considered only, disregarding effect from friction between layers and interaction with adjacent slabs. Furthermore, symmetry conditions is applied considering only one quarter of the slab. Orthogonal cracks is modelled by inserting a longitudinal cohesive zone a with 45° angle between the symmetry-lines, in addition to an arch cohesive zone close to the centre of the slab (distance=50 mm). The arch cohesive zone was inserted to avoid numerical issues. An overview the structure can be seen in the sketch in in Figure 3.


Figure 3. *Sketch of model geometry applied in the sensitivity study*

Preliminary analysis show that the structure outlined in Figure 3 sufficiently captures the effect from the orthogonal cracks in the full slab.

4.1 Effect of slab dimensions and CBM thickness

In traditional methods for pavement design layer thickness is an important parameter, increased to limit the stresses in underlying layers. Furthermore, it is evaluated that the slab dimensions, or in other words, distance between aggregate interlock joints, is an important parameter, as this parameter will influence the bending behaviour of the structure.
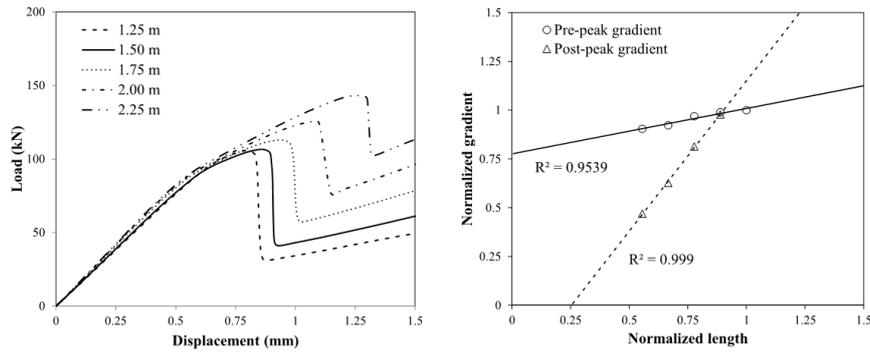
Figure 4. *To the left: Load-displacement curve for CBM-slab length varying from 1.25-2.25m (2.5-4.5 m in full model) keeping thickness constant (250 mm). To the right: Normalized pre-and post-peak gradient versus normalized slab-length*

From the load-displacement curve, shown in Figure 4, it can be observed that all models behave similarly with close to identical gradient on the linear part of the pre-peak curve. Peak-load and peak-load displacement increases with increasing length of the slab before unloading occurs. Furthermore, it can be observed that there is a significant effect from bending; the post-peak response of the structure being highly dependent on the length of the slab.
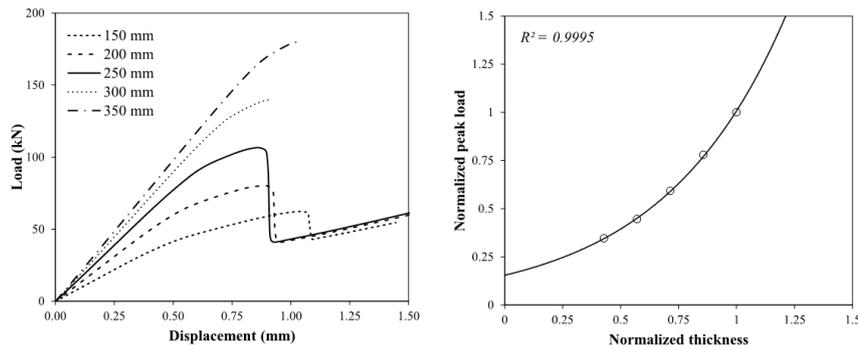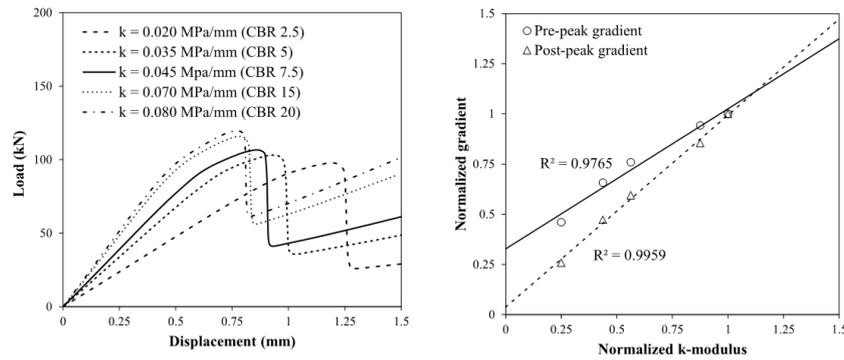

Figure 5. *To the left: Load-displacement curve for CBM thickness varying from 150-350 mm keeping length/width constant (3 m in full model). To the right: Normalized peak-load versus normalized thickness curve*

From the load-displacement curve, shown in Figure 5, it can be observed that the pre-peak stiffness of the structure is increasing with increased thickness. The peak-load is reached in the same region of displacement for all models. Thereafter the longitudinal crack opens at the end of the slab, unloading occur, and the post-peak strength of the structure is reached. The post-peak response of the CBM is mainly controlled by the stiffness of the subgrade soil and the length of the slab.

4.2 Effect of k-modulus

Another important parameter in traditional pavement design is the stiffness of the unbound- sub-base and subgrade soil. In slabs on grade structures, normally defined by a spring stiffness or modulus of subgrade reaction (k-modulus). The variation in k-modulus applied is used to represent the stiffness of a high-quality sub-base layer with thickness of 150 mm over a subgrade of varying quality (California Bearing Ratio 2.5-20).
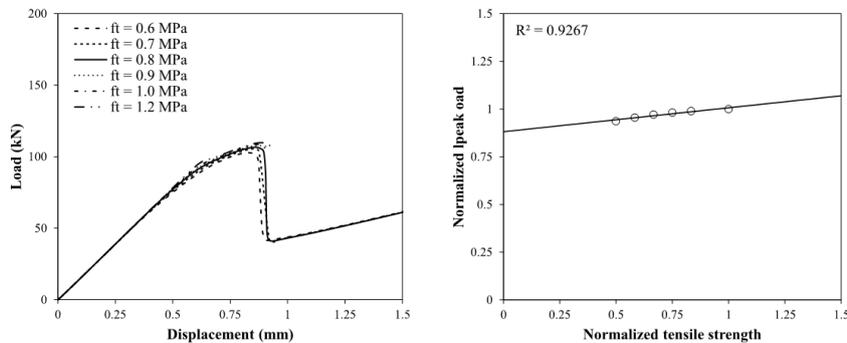
Figure 6. *To the left: Load-displacement curve for k-modulus varying from 0.02 to 0.08MPa/mm. To the right: Normalized pre- and post-peak gradient versus normalized k-modulus curve*

From the load-displacement curve, shown in Figure 6, it can be observed that increasing stiffness of the support results in both increasing pre- and post-peak gradient on the load-displacement diagram as expected. The relation is close to linear, especially for the post-peak response as there are no nonlinear effects from the crack in this phase.

4.3 Effect of tensile strength and fracture energy

The two main material parameters influencing the fracture process of the CBM are the tensile strength and the fracture energy.

Figure 7. *To the left: Load-displacement curve for tensile strength varying from 0.6 to 1.2MPa keeping fracture energy constant. To the right: Normalized peak-load versus normalized thickness curve*

From the load-displacement curve, shown in Figure 7, it can be observed that the effect of variation in tensile strength is small, both with regard to peak-load and pre- and post-peak response, this can be explained by the fact that crack initiation occur at a displacement of approximately 0.2 mm. Thereafter the response is a primarily controlled by geometry, and other material properties, i.e., the stiffness of the supporting layers and fracture energy.
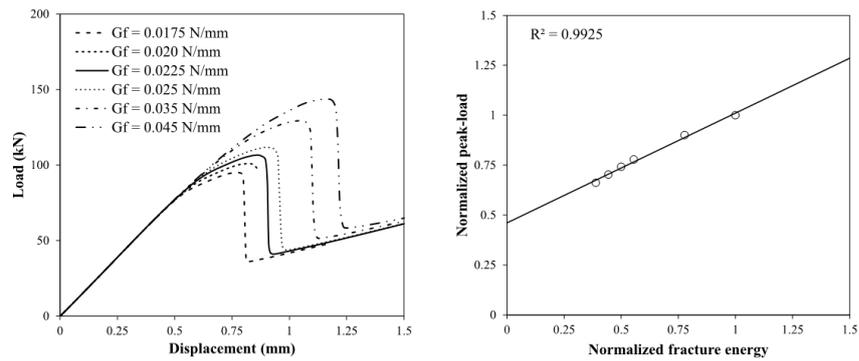
Figure 8. *To the left: Load versus displacement curve for fracture energy varying from 0.0175 to 0.045 N/mm. To the right: Normalized peak-load versus normalized fracture energy curve*

From the load-displacement curve, shown in Figure 8, it can be observed that the there is a significant effect from the variation in fracture energy on the peak-load, with a close to linear relationship on the normalized peak-load versus fracture energy curve.

5. Numerical analysis of full scale composite block pavement structure

To extend the analysis to more realistic pavement systems, numerical analysis of a full slab ($3.0 \times 3.0 \times 0.3$ m³) subjected to interior container casting loading (0.178×0.162 m²) is carried out.

The response of the composite concrete block pavement structure is mainly controlled by the cemented base layer and the subgrade soil. The properties and thickness of the concrete block pavers does hardly influence the overall response and bearing capacity of the pavement structure (Huurman 1992), since the container castings produce a close to rigid body movement of the stiff concrete blocks over the soft layer of bedding sand, which is unable to absorb any significant bending moments.

Thus, for the present study the response from CBP surface and container casting load is simulated using a simplified approach, placing unit displacements over an approximated area, i.e., the area of blocks in contact with container castings, directly on top of the bedding layer. The method is verified by linear elastic analysis, comparing the simplified approach with a full model, considering both block, jointing-and bedding sand, as shown in Figure 9.
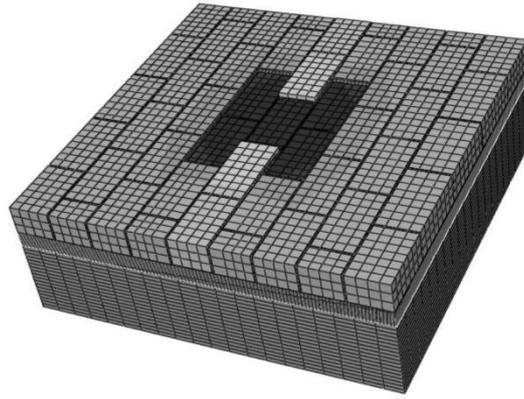
Figure 9. *Surface displacement of full concrete block pavement model used for validation of modelling technique*

From the comparison between the full model and the simplified approach applied in the present study, shown in Figure 10 (a) to (c), it can be observed that good agreement is obtained for the response of the CBM (Figure 10 (a) and (b)). The method also gives an adequately good prediction of the surface displacements, (Figure 10 (c)).


(a)

(b)

(c)

(d)
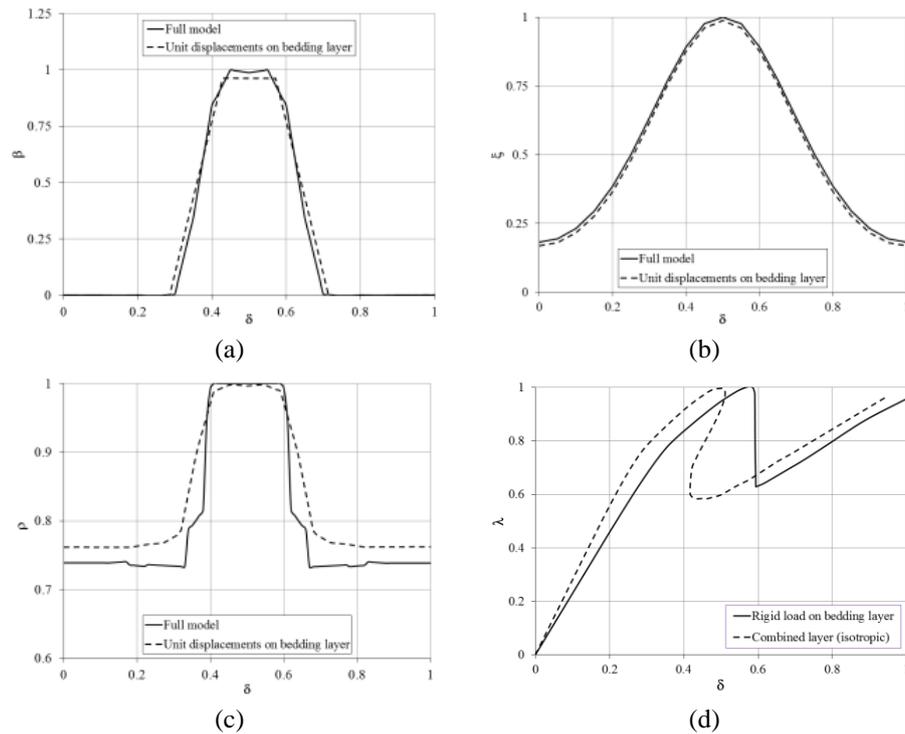
Figure 10. *Comparative study evaluating the responses of a simplified CBP pavement; (a) normalized vertical stresses (β) on top of CBM, (b) normalized maximum principal stress (ξ) at the bottom of CBM, (c) normalized surface displacements (ρ) and (d) normalized load line displacement curve for the approach applied compared to other modelling techniques, e.g., placing the rigid load (0.178×0.162 m2) directly on top of a combined homogenous layer (0.356×0.324×0.11 m³), representing the CBP's, jointing-and bedding sand.*

The methodology applied may introduce numerical issues for the contact between bedding sand and CBM due to the high stiffness ratio between materials,

making it difficult to obtain convergent solutions and/or a total description of the equilibrium path, e.g., snap-back during unloading. If the latter is important to the analysis, further simplification of the model should be considered in order to limit the computational cost, as shown in Figure 10 (d).

Model parameters shown in Table 3 are applied, using a k-modulus of 0.035 MPa/mm (CBR 5). Normal- and shear forces in aggregate interlock joints are neglected as their effect on the load-displacement curve can be assumed small for interior loading.

(a)

(b)

(c)
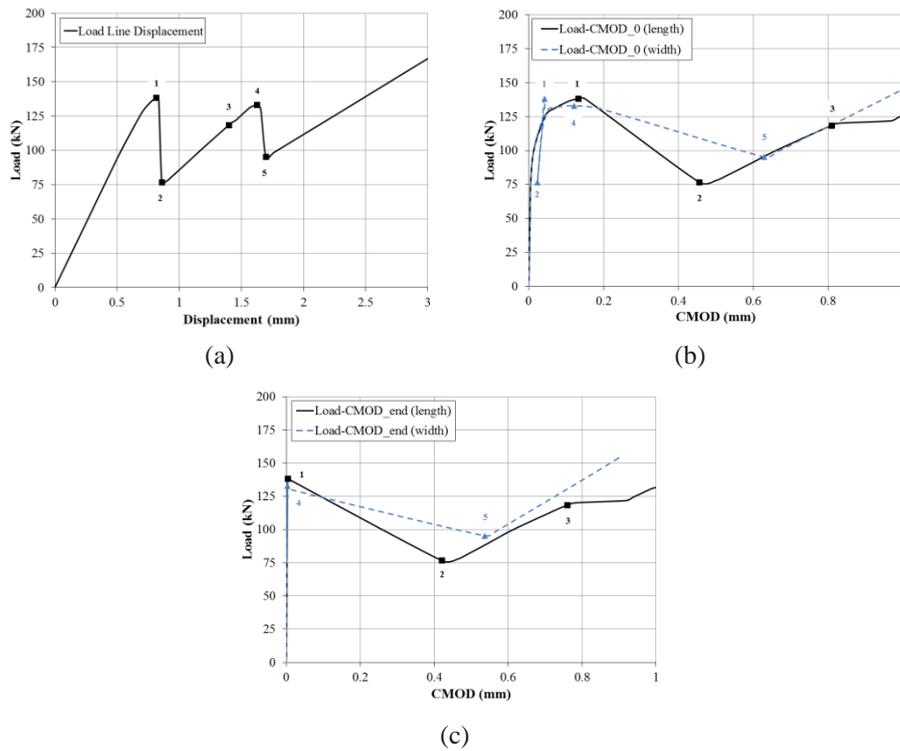
Figure 11. *Presentation of numerical results: (a) Load Line Displacement (LLD) curve of full slab response on elastic foundation, (b) Load-CMOD curve for the cohesive zone at the slab bottom centre and (c) Load-CMOD curve or the cohesive zone at the slab bottom edge*

From the load-displacement curve, shown in Figure 11 (a), it can be observed that the load-displacement curve has two peaks (load point 3 and 4). This behaviour can be explained by the rectangular load configuration, resulting in slightly higher principal stresses in one of the two directions. From the Load versus Crack Mouth Opening Displacement (CMOD) curve, shown in Figure 11 (b), it can be observed that cracks in both directions are initiated at a load magnitude of 75 kN, damage of the cohesive zone then progress toward the edges of the slab. At load level point 1, nodes at the bottom of the slab in length direction (shortest direction) have exceeded the final (zero traction) displacement, resulting in the unloading of the load-displacement curve, whereas the crack in the width closes (load level point 1 to 2) and then remains stable until the second peak at load level point 4. At load level point 3 all nodes in the length direction have exceeded the final displacement, as shown in Figure 11 (b) and (c), resulting in the snap on the curve.

Finally, it can be seen, that the problem to be solved is highly nonlinear, and that direct comparison with presently available design guidelines, e.g., Interpave (2008), makes little sense as the allowable load levels are twice the magnitude compared to the peak-loads found in the present study.

6. Conclusion

The use of a cohesive contact formulation for simulating the fracture in the CBM-layer in a simplified three-layered composite block pavement has been investigated by studying the main parameters that affect the responses of the pavement structure

Testing of the model on CBM-beams show that application of the cohesive model is promising to description of the fracture behaviour of CBM-materials. However, tests results are limited and further analysis and testing is necessary to fully evaluate the applicability of the cohesive model.

The effects from the variation in CBM-thickness and slab dimensions proved to be important parameters. The peak-load was highly influenced by thickness, whereas slab dimensions proved to be a main controlling parameter of the post-peak response of the structure. Furthermore, it can be concluded that the fracture process is more affected by the fracture energy than the tensile strength.

The full slab model shows that cracking is initiated at an early stage. It is also found that the peak-loads in the present study are significantly lower than allowable load levels given in presently available guidelines for composite block pavements. Evaluation of the full bearing capacity of the structure can be done with the methodology implemented, e.g., by including a yield criteria for the subgrade soil.

The present study shows that a cohesive model with linear softening adequately describes the fracture behaviour of CBM. Moreover, computationally fast FE models were developed, applicable for engineering applications. It is envisaged that the methodology implemented can be extended to more complex and realistic problems, e.g., including analysis of loading positions, cyclic loading and aggregate interlock behaviour, for development of more rational failure criteria in pavement engineering.

7. Bibliography

Hillerborg, A., Modéer, M., and Petterson, P-E. 1976. Analysis of crack formation and crack growth in concrete by means of fracture mechanics and finite elements. Cement and Concrete Research. 6(6): 773-781.

Riks, E. 1979. An incremental approach to the solution of snapping and buckling problems. International Journal of Solids and Structures, 15(7): 529-551.

Hilsdorf, K.H, Brameshuber, W. 1991. Code-type formulation of fracture mechanics concepts for concrete. Journal of Fracture, 51: 61-72.

Huurman, M., Houben, L.J.M. and Kok, A.W.M. 1992. Development of a three-dimensional finite element model for concrete block pavements. In Proceedings Fourth International Conference on Concrete Block Paving, Auckland, New Zealand, Volume 1, pp. 89-98.

Shahid, M. A. and Thom, N. H. 1996. Performance of cement bound bases with controlled cracking. In RILEM PROCEEDINGS (pp. 55-64). CHAPMAN & HALL.

Theyse, H. L. and De Beer, M. and Rust, F. C. 1996. Overview of South African Mechanistic Pavement Design Method. Transportation Research Record, 1539: 6-17.

Meda, A., Plizzari, G.A., and Riva, P. 2004. Fracture behavior of SFRC slabs on grade. Materials and Structures. 37(6): 405-411.

Thøgersen, F. Busch, C. and Henrichsen, A. 2004. Mechanistic Design of Semi-Rigid Pavements - An incremental Approach, Danish Road Directorate, Report 138

Roesler, J.R., Paulino, G.H, park, K., and Gaedicke, C. 2007. Concrete fracture prediction using bilinear softening. Cement and Concrete Composites, 29(4): 300-312.

Knapton, J. 2008. The structural design of heavy duty pavements for ports and other industries. Interpave, Uniclass L534, Leicester, United Kingdom

Yeo, R. 2008a. Fatigue Performance of Cemented Materials under Accelerated Loading – Influence of Vertical Loading on the Performance of Unbound and Cemented Materials. TT1065, Austroads Technical Report AP–T102/08, Sidney, Australia.

Yeo, R. 2008b. The Development and Evaluation of Protocols for the Laboratory Characterisation of Cemented Materials. TT1065, Austroads Technical Report AP-T101/08, Sidney, Australia.

Gaedicke, C., and Roesler, J.R. 2009. Fracture-based method to determine the flexural load capacity of concrete slabs. FAA-05-C-AT-UIUC, Department of Civil and Environmental Engineering, University of Illinois, Urbana, Illinois.

Aure, T.M., and Ioannides, A.M. 2012. Numerical analysis of fracture process in pavement slabs. Canadian Journal of Civil engineering, 39(5): 506-514

ABAQUS. 2013. Analysis user's manual, Version 6.13-1, Dessault Systems, Providence, R.I.

BS EN 14227-1:2013. Hydraulically bound mixtures. Specifications. Cement bound granular mixtures, British Standards Institution